"THERMAL BEHAVIOR OF BIMA ANTENNA DISH STRUCTURE"

Jingquan Cheng

September 19, 1995

NO. 141

Thermal Behavior of BIMA Antenna Dish Structure

Jingquan Cheng
Sept. 19, 1995

An important characteristic of the 6 m diameter antennas of the BIMA Array at Hat Creek is that their structures, including their dishes and feedlegs, are all made of steel resulting in low cost and simple construction techniques. However, steel has a relatively large thermal expansion coefficient($1.2 \times 10^{-5}/^{\circ}C$)and to avoid temperature-related problems, the base, yoke, dish support ring and dish structure of the BIMA antennas are all protected by simple sunshades (foam and aluminum skin). These sunshades are separated from the structure by a thin air gap. Small gaps between sunshades also exist, mainly to help avoid heat build-up inside. The feedlegs of the antennas are also protected by aluminum foil. Forced air flow is provided inside the feedlegs and the output air flow from the feedlegs is used to cool the secondary mirror(during solar observation, the secondary mirror is hot even with the air cooling). The dish section, which is enclosed by the sunshades, also contains four high-power air circulation fans to stir the air inside the structure and in order to provide heat exchange with the envoriment some air flow through the gaps of the sunshades is permitted. This is a new thermal control method in millimeter wavelength antenna design. The exact analysis of thermal problems is very difficult, in particular defining the temperature distribution on the structure. Fortunately, in late June, 1993, J. W. Lamb and J. R. Forster(1993) made systematic temperature measurements on the BIMA dish structure and these measurements provide a base for the analysis in this memo. The measured temperature distributions combined with the TIW Nastran tipping structure model are used to predict the pointing and surface accuracy of the BIMA antenna and this analysis is extended to predict the performance of an 8m diameter antenna suitable for use in the MMA.

1. Typical thermal pattern of the BIMA dish structure.

The main source of thermally induced dish distortion is solar radiation. Site temperature change plays a less important role. The maximum and minimum solar loading on a high altitude site is about 1260 W/m^2 for perihelion and 1140 W/m^2 for aphelion. The solar loading on the dish is determined by the absorptivity of the surface, the air mass of the solar path and the angle of the dish surface relative to the solar beam. The absorptivity of the surface varies with its material and surface finish. For a polished aluminum surface(such as anodized surface) it is 0.04-0.06. For a rough surface(new sunshade and new panel surface), it is 0.07. However for an oxidized surface(aged sunshade, aged panel surface and the back surface of the panels) it could be as high as 0.2-0.33. The main heat input of the dish is from the panel front surface. The sunshades reflect most of the solar energy. The heat absorbed by the panels is partly radiated to the sky, partly removed through natural convection from the front, partly stored inside the panels resulting in a temperature increase and the remainder will be passed to the backing structure through radiation from the back of the panels and through forced convection inside the dish(the sunshades on the

dish block the radiation from the back surface of the panels). The absorptivity and emissivity of the surface are usually equal for a given material. Under the solar loading(daytime), the temperature of the panels is higher than the ambient temperature(about 10-14 ° C, Greve recorded a panel ambient temperature difference of 15-19 °C for IRAM 30 m antenna(Figure 5, which is from Greve, 1992, Fig 2.4)). The thermal input of the backing structure is from the radiation of the panels and from the forced convection passing through the back of the panels. The thermal output of the dish structure is by the forced convection of the fresh air from the sunshade gaps. Under solar loading, the backing structure temperature is lower than the panel temperature but it is still higher than the ambient temperature. Since the panel orientation relative to the sun is complex, the temperature increase of the backing structure is always not uniform(central cone which has a larger thermal time constant is also a reason for thermal gradient within the dish). This in turn produces the most harmful rms spatial temperature deviations. When the solar loading is removed, the only heat transfer of the backing structure is the radiation through the front surfaces of the panels and through the forced convection inside the dish. The main heat source at this time is from the central cone which has a temperature lag. The temperature of the backing structure will decrease and finally stabilise when the cone and backing structure temperatures are equal. At this time the temperature of the backing structure may be a little lower than the ambient temperature due to the structure radiating to the cold sky.

Figure 1 shows the measured average backing structure temperatures and their rms spatial variation(Lamb and Forster,1993)over several days. The temperature is measured over 32 positions on the backing structure when the sunshades were in place and the fans were on(ref. Figure 3). This figure does not give the environment temperature changes, which has a much smaller amplitude and also has a phase lag(ref. Figure 5, which is from Greve, 1992, Figure 2.4). The rate of the average backing structure temperature change is about 3°C per hour(In the following tables, the rate of dish temperature change used is 1.5 °C/30 minutes). From the figure, the rms temperature variation of the backup structure involves two distinct but consistant parts: one is smooth and the other has a half sine curve shape. The rms value of the smooth part is small(0.2° C rms) and it starts from the time when the peak of the average temperature is reached and finishes at the time when the bottom of the average temperature is reached. The half sine curve part is larger(0.6° C rms) and it starts from the time when the bottom of temperature is reached and finishes at the time when the peak of the average temperature is reached. Occasionally, some very large deviations could be found. These very large values range from 0.9 to 1.2°C rms and appear to be randomly distributed. The figure reveals that for a shielded structure, the temperature of the dish is(or nearly is) independant of the wind at the site.

Figure 2 is the spatial distribution of dish temperature with time for one day. The lowest tempertature of the measured day was 10.7 °C and occurs at 102 hour. In two hours, the dish temperature increased to 15.7°C and after another two hours, it reached 19.8°C. From 106 hours, there was significant temperature scattering within the backing structure. The bottom trusses(represented by dotted lines in Fig. 2) were cooler than the top trusses and the central bottom ring near the cone showed a temperature lag. At 112 hour, the top and bottom dish temperature were mixed and the variations were smaller. For the 24 hour period greater spatial temperature variations occured at 106-118 hours and lower ones at 102-104 and 120-124 hours.

In the analysis of this memo, we choose three typical day time values those are at 106, 108 and 110 hours.

2. Surface deformations calculated by using measured data.

By incorporating the TIW structure model, the surface shape of the dish can be calculated for any temperature distribution. In the dish structure there are only 32 measured points, but linear interpolation is used to generated intermediate temperature values. Fig. 3 shows the geometry of the backup structure. Temperature data for the tripod support points are derived by subtracting 0.2° C from the temperature of the nearest points. This is done because these points are outside the dish structure and they may subjected to more environmental cooling. The temperature used for the rest of the points on the structure, including cabin, feedlegs and most of the dish's central cone, is called the "reference temperature". The reference temperature used is an average of the temperature data for the inner bottom ring. In this way, it ensures that the cabin, the ring, central cone and feedlegs have no(or very little) effect on dish thermal distortion in the analysis.

The analysis is then carried out for three typical daytime hours. These are during the times of hours 106, 108 and 110. At hour 106 the temperature deviation of the backup structure is 0.55° C rms, which is slightly smaller than the typical value of 0.6 ° C rms for day time. The following table lists the analysis conditions and results. These are the reference temperature, the rms surface deviations before and after surface fitting, the change in focal length if the best fitted paraboloid is applied and the z displacement(along the dish surface axis) of the dish vertex due to the thermal distortion. In the 110 hour, nearly all the numbers are larger. This case may be a typical case for the daytime condition.

Tabble 1 Surface rms errors of three daytime hours*

Time in Hours	Ref. Temp.	rms Surface Error Before Fitting	rms Surface Error After Fitting	Focal Length Change of the Fitted Paraboloid	Vertex Displacement in z Direction
106 hr	19.0° C	16 μm rms	5 μm rms	+112 μm	+6 μm
108 hr	21.0° C	21 μm rms	5 μm rms	+142 μm	+7.6 μm
110 hr	23.5° C	18 μm rms	6.5 μm rms	+256 μm	+123 μm

* all the linear numbers in this and following tables are peak values, all rms values are written with rms.

In the above table, column three shows the thermal induced surface rms errors(In table 5 the dish surface error uses 18 μm rms). The thermal gradient induced phase rms errors should be twice these numbers(In table 5 the dish phase error 1 uses 40 μm rms). The vertex displacement will also affect the phase error of the central rays. In table 1, the rms temperature devations are about 0.6 ° C. If the maximum temperature devation(eg. a deviation of 1.2 °C) of the backing structure, which is always happening in a very short time scale, is used, the rms surface devation may be

larger(about 32-34 μm). These errors are all relative numbers, since the absolute temperature change is not considered. Another big factor in increasing the dish surface error is the temperature difference between the dish and the cabin, which will be discused in the later sections.

3. Deformation under absolute temperature change.

For any antenna structure, an absolute temperature change will result in simply a change of scale resulting in a change of focal length. The calculation results of a 25°C (a typical number for daily dish temperature variation) and a 1.5°C (a typical number for a 30 minute temperature change of the dish) difference on the dish structure temperature are as follows. In this calculation, the surface nodes have been checked on a paraboloid surface. The rms error after the best fit in the table may be caused by rounding error in the computation.

Table 2 Surface error under absolute temperature change

Temperature Change	rms Deviation	rms After Fitting	Focal Length Change
+ 25 ° C	162 μm rms	0.5 μm rms	+749 μm
+ 1.5° C	9.8 μm rms	0 rms	+45 μm

From this calculation, long term temperature change will cause phase changes so requiring phase calibration on a nereby calibration source. An important question is how often will the calibration be needed. Here we attempt to calculate this for the measured conditions on the BIMA antennas. The thermal conditions of the antenna are complicated. Depending on the thermal time constants, all parts of the antenna have different temperatures at different times during periods of temperature change. The larger the time constant, the smoother the temperature curves are. The temperature of the feedlegs is also variable. However, one can derive a general formula for the phase change. In the case the reciever is fixed with the vertex of the dish, the net phase error is: $3\delta_1$-$2\delta_2$, where δ_1 is the displacement of the primary dish and δ_2 is the displacement of the secondary mirror. If the reciever is fixed itself, then the phase error is $2\delta_1$-$2\delta_2$. Taking the displacement of the primary mirror to be zero, the net phase error due to absolute temperature change is twice the focal length change, that is 60 μm/°C(In table 5 dish phase error 2, using 1.5 °C temperature change, the peak error is 90 μm and the rms error is 30 μm). Considering the expansion of the dish itself, the primary mirror also moves forward so reducing the phase error. The unknown problem here is: Do the feedlegs keep the same temperature as the dish temperature? If it is not true, then the 60 μm/°C phase error number for the dish part will vary considerably. A 1°C temperature difference between the dish and the legs will cause the secondary mirror to move 72 μm (assuming the feedleg length is 3.354 m for a 6 m dish) inwards or outwards axially, resulting a phase error of 144 μm/°C(In table 5, the feed error using 1.5° C of the number, the rms error is 70 μm). So the combined phase error may be a lot larger.

The above calculation is for a steel backing structure with steel feedlegs. When the feedlegs are made of other material, such as CFRP, the effect is the same as the case when there is a difference between dish and feedleg temperature. The phase error is then 144 μm/°C.(In table 6, the 8 m feedlege error using 144μm/°C x 1.5°C x 1.33/3 =95 μm rms ,where 1.33 is a scaling factor from 6 m to 8 m and the factor 3 is used for estimating the rms value from a peak value.).

4. Pointing changes calculated by using measured data.

Pointing change is caused by a number of factors. These are displacement of the dish vertex dv, displacement of the secondary mirror ds, the rotation of the secondary mirror relative to the primary dish ω. The formula for the pointing error is:

$$ó = dv/f + k_p\ ds/f - k_s/M\ ds/f - 2c/f\ k_s\ \omega/M$$

where f is the primary focal length;
k_p is primary beam deviation factor;
k_s is secondary beam deviation factor;
M is magnification factor;
c is the distance between primary and secondary focii.

By using the numbers for the BIMA antenna(c and M use estimated numbers), f =2.56 m, k_p = 0.88, k_s = 1, 2c = 6 m, M = 28.6, the biggest contribution to the pointing is from the displacement term of the secondary mirror ds, which has a factor of 0.069 arc sec/μm. The displacement of the secondary mirror is caused by two factors: one is the thermal deformation of the dish only and the other is from the thermal deformation of the feed leg. In the previous calculation, we assumed the feed legs having the same reference temperature. The dispacements of the secondary mirror under this condition in x and y directions(z axis is through dish axis) are listed in the following table for the thermal distribution of 106 and 108 hours.

Table 3 Dish thermal induced secondary mirror movement

Hours	dx	dy	ds
106 hours	+13.5 μm	+2.7 μm	13.7 μm
108 hours	-15.8 μm	-6.1 μm	16.9 μm

By converting the displacement data into pointing errors, the peak pointing error caused by the dish thermal deformation is 0.95 arc sec at 106 hour, and is 1.15 arc sec at 108 hour(In table 5, the dish pointing error uses 0.4 arc sec rms). Since the data of dx and dy of both cases have opposite sign, the actual pointing change is at lest 2.1 arc sec during 2 hours interval. The best rate of changing in pointing is 1.05 arc sec/ hour.

The secondary mirror position could also be affected by the thermal deformation of the feedleg if the feedleg is made of steel. The position of the secondary mirror will change if there is a thermal difference between feedlegs. The worst condition of the feed leg caused pointing error is when one of the feed legs has a higher temperature than the rest. The BIMA antenna has three feedlegs, one is at the top and the other two are 90° apart at the bottom. The calculated effect of the feedleg thermal deformations by 1 °C diffenerce is as follows:

Table 4 Feedleg thermal induced secondary mirror movement.

Feedleg position	dx	dy	ds
Top feedleg is 1°C higher	0 μm	-26.4 μm	26.4 μm
One of the bottom feedlegs is 1°C higher	+33.8 μm	+14.9 μm	36.9 μm

The corresponding feedleg induced thermal pointing errors are therefore 1.8 arc sec to 2.5 arc sec/°C for the feedleg temperature difference(In table 5, the feed pointing using 1.5 °C number of 4 arc sec peak value which is 1.3 arc sec rms.). For a four feedleg secondary support structure, the effect of one feedleg being 1°C higher is a displacement of 25 μm. which equals a pointing error of 1.7 arc sec.

The feedlegs of the BIMA antenna have shiney aluminium sunshades and they are also cooled by outside air pumped from the bottom of the legs. The heat exchange of the feedleg includes solar radiation, radiation to the sky and the forced convection of the air flow. Shiney shades have a lower absorption and emissivity(may be near 0.04), which minimises the absorbtion of solar radiation. Even so, the solar loading is still the main cause of the feedleg thermal difference. The worst temperature difference between feedlegs may be 2-3°C(assuming a similar temperature variation as the dish) resulting in a significant pointing problem.

The combined effect from the dish and the feedleg is complicated. However a worst case is that the dish is heated by the sun on one side from the front and the feedleg is heated by the sun from the other side(since the back of the dish is all insulated). In this case, the pointing errors of the two parts will be added together. For reducing the pointing error, CFRP feed leg is very effective.

5. Other techniques for dish thermal control.

There are several techniques for dish thermal control of outdoor antennas. The simplest way is represented by the 10 m Leighton telescopes at Owens Valley Radio Observatory(OVRO). It is an open, flat structure (The Leighton dish also uses small cross-sectional members to reduce the thermal time constant). The structure is very open and it will be in thermal equilibrium with the

air in winds as low as ~5 m/s. D. Woody(1994) stated that a flat dish produces less rms distortion. His calculation shows a gradient of 1 K across the diameter produces only a 3 μm rms distortion for the Leighton dish. This number of a 10 m OVRO dish is smaller than the calculation of a typical 8 m dish, which is 7.5 μm before fitting and 1.8 μm after fitting (Cheng, 1994). Cheng's calculation shows that a 1 K gradient between front and back produces 44 μm rms error before fitting and 8.7 μm error after fitting. A 1°C gradient radially produces 12 μm and 8 μm before and after fitting. The troublesome distortion of the Leighton 10 m dish is the temperature difference between the dish and mounting frame, which produces a 7 μm rms distortion per degree difference. In the next section, we will find that the cabin temperature change has a strong effect on the rms error for the BIMA antenna. The measured temperature difference on the 10 m dish is typically less than 1° C, with a worst case value of 5°C. In conclusion, the estimated distortions of the Leighton dish are typically less than 10 μm rms, with a worst case of 35 μm. (Note: for an 8 m typical dish, the rms should be about 13 to 40 μm rms.)

The second technique of thermal control is represented by IRAM's 15 m telescopes. This involves no active thermal control. The dish of the telescope is a mixed CFRP (horizontal) and steel (vertical) structure to accommodate the steel central hub. The backup structure is in a closed volume. Natural air flow through small louvers helps to avoid condensation. The back surface of the backup structure is covered with a layer of radiation shielding. The radiation shield consists of two aluminum plates (~1 mm thickness each) separated by 5 mm and connected by corrugated aluminum. The shield's outer surface is covered with high reflectivity aluminum foil. The panels on the front of the dish are made of honeycomb CFRP. Greve(1992) gives the measurements of average inside temperature, rms variation of inside temperature and maximum temperature deviations of upper and lower sections inside the dish volume. The measurements show that the average temperature inside is the same as ambient temperature during the day and, at night, it is significantly lower (by 5° C). The rms of temperature variation is 0.8-1.0° C during the night and 2-3° C during the day. A significant phenomenon is the vertical temperature gradient inside the volume. The difference is ~2° C for night and ~10° C for day. The CFRP members reduce distortion greatly. The calculated distortion of the 15 m IRAM dish is of the order 8 μm.

A combination of insulation and ventilation is used at the IRAM 30 m antenna. All of the antenna structure parts which are made of steel, including backing structure, yoke and feedleg, are insulated with Polyurethane foam and white TiO paint. The backing structure is fully sealed. Inside the backing structure, a tangential air flow of several m/s speed is provided, with the air either being cooled or heated (25 - 40 kW respectively.) The feedlegs are also temperature controlled. The temperature of the yoke is used as a reference for active temperature control. Fig. 4 shows the rms temperature change inside the backing structure during active thermal control. The average rms is about 0.2-0.6 °C, but it could reach 1.2° C in a worst case scenario. In the IRAM 30 m antenna, the temperature difference between the yoke and the backing structure is only about 0.5° C. However, this type of antenna thermal control is costly.

6. Discussion of BIMA dish thermal distortion.

From the point of view of measured temperature gradient, compared to IRAM's costly method of heating and cooling its 30 m antenna, BIMA's thermal control technique is very effective. The gradient during the day is about 0.6° C rms, with a worst value of about 1.2° C (it is estimated that the worst case value for the Leighton dish is 1.6° C, for IRAM 15 m dish it is 3.3° C and for IRAM 30 m dish it is 1.2 °C). The only thing which is superior for IRAM 30 m antenna is that the temperature diffferenece between yoke, cabin, dish and feedleg is very very small. In this memo, the calculation of the surface rms deviation is based on the best conditions for the measurement; that is, a smooth temperature fitting between the measured points on the dish and a uniform hub (supporting ring) and cabin temperature which is equal to the average value of the back surface inner ring points. However the question arises as to what the measurements would be like in the worst possible conditions. To answer this question we need to consider three scenarios. The first one concerns the problem which occurs when the temperature distribution between the measured points is not smooth. The second scenario involves a temperature difference between the dish, cabin and the center cone. The third is the case when the ring and central cone themselves have a temperature gradient. These are questions which are difficult to answer exactly.

Some analysis had been done in order to understand the first of these three questions. Since there are not enough temperature data for the dish structure analysis, instead of using a smooth fitting temperature data for the girds in between, we used the measured temperature data from two perpendicular ribs for all the five ribs in between consectively. Surprisingly, calculations show that the rms deviations both before and after fitting remain unchanged. This was done at the time of 106 hours; the results before and after fitting are 16 μm rms and 5 μm rms, respectively. It seems as far as the temperature difference remains unchanged, the surface rms error will be the same. High spatial frequency does not increase overall rms errors.

For the second question, calculations were performed for a reference temperature(Note: reference temperature in the calculation is the given temperature for the cone and cabin) which is 1° C and 2° C lower than the average temperature of the dish inner bottom grids. The analysis shows a large increase in rms errors when the reference temperature changes. For a 1° C decrease of the reference temperature at the time of 106 hours, the rms errors will be 32 μm rms and 8 μm rms(from 16 μm rms and 5 μm rms) before and after fitting. For a 2° C decrease, the numbers will reach 40 μm rms and 10 μm rms, respectively. The rate of change in rms surface error is about 14 μm rms/°C(In table 5, the cabin surface error using 14 μm rms.). However, if the cabin's temperature is increased by 1° C, the rms results are lower than the result shown in Table 1. Of course, if the cabin temperature is too high, the rms will increase again. Here the question becomes "is there a temperature difference between cabin, cone and dish structure?" Unfortunately, there are no measurement results which we can use to determine the answer to this question. Bregman and Casse(1985) reported a temperature lag of 5 °C between main frame and backing structure of the JCMT antenna. With partial insulation of the cabin and forced convection around the central cone, the thermal lag may be reduced but a temperature lag of 2-3°C is expected. This increased the surface error to a level unacceptable for higher frequency work.

We have not done analysis on the third case. But a change of the rms values is expected when the support ring is not at the same temperature as the cone. In the BIMA antenna design, the dish support ring is shielded by a sunshade, but the cabin (with surface painting) is exposed to the environment. This design is intended to keep the cabin temperature identical to the environmental one and to avoid the temperature difference around the ring. However, from the measured data, there is a temperature scattering of the innermost back points which are located immediately to the support ring (see Fig. 2). The measured scatter is about 1-1.5° C. This scattering should be a reduced value of the thermal gradient around the support ring, in spite of the fact that a sunshade shielded the ring.

7. BIMA dish errors and the 8 m scaling up.

To understand the thermal performance of a steel dish is a difficult task. We still need more measurements and analysis. However, from the discussion in this memo, we can sumarise our best estimate of the thermal errors for the BIMA antenna. These errors include surface error, pointing error and phase error. Since refocusing, pointing calibration and phase calibration are routine practices in the millimeter observation, we therefore need to consider the potential performance of the steel dish when these routine practices are applied. The following table is a summary of the BIMA dish performances at daytime. The numbers listed are our best guess for the thermal errors based on measurements and analysis.

Table 5 Summary of daytime BIMA dish thermal errors.

	Surface Error	Pointing Error	Phase Error
Themal condition	rms dish deviation: 0.6° cabin dish difference: 1°C	rms dish deviation:0.6°C feedleg difference: 1.5°C	rms dish deviation:0.6°C feed dish difference:1.5°C
Absolute error in 30 minutes	dish error 18 μm rms cabin error 14 um rms total rms 23 μm	dish error 0.4 arcses rms feed error 1.3 arcsec rms total 1.4 arcsec rss worst case1.7 arcsec rms	dish error 40 μm rms* dish error 30 μm rms** feed error 70 μm rms total 20-100 μm rss
Rate of change	14 μm rms/ hr	2.5 arc sec /hr	40-200 μm/ hr rms
Error after calibration	23 μm rms	2.5 arc sec peak value 0.9 arc sec rms calibration every 30 min	4-10 μm rms calibration every 3 min

* This term is caused by the temperature spatial distribution on the dish.
** This term is caused by a 1.5°C temperture change of the the dish.

Table 6 The thermal performance of a scaled 8 m steel dish with CFRP feed leg design

	Surface Error	Pointing Error	Phase Error
Themal condition	rms dish deviation: 0.6° cabin dish difference:1°C	rms dish deviation:0.6°C feedleg difference: 1.5°C	rms dish deviation:0.6°C feed dish difference:1.5°C
Absolute error in 30 minutes	dish error 24 μm rms cabin error 18.5 μm rms total rms 30 μm	dish error 0.4 arcsec rms feed error 0.1 arcsec rms total rms 0.4 arc sec	dish error 52 μm rms* dish error 40 μm rms** feed error 95 μm rms total 115 μm rss
Rate of change	18 μm/ hr	1.0 arc sec /hr	230 μm/ hr
Error after calibration	24 μm rms	0.5 arc sec peak value 0.2 arc sec rms calibration every 30 min	12 μm rms calibration every 3 min

* This term is caused by the temperature spatial distribution on the dish.
** This term is caused by a 1.5°C temperture change of the the dish.

This memo discussed the erorrs of the BIMA 6 m dish at day time. A dominant error term is the pointing. The dish and feedleg induced pointing errors are always added up in the worst case. This limits the performance of the operation. By scaling BIMA dish to 6 m, not only the pointing is a problem, but also the weight from the steel feedleg becomes a burden in the dish design. Therefore, it is desirable to use CFRP feedlegs. By scaling up from a 6 m dish to an 8 m dish, the linear terms will all increase by 33% if the thermal gradient remains unchanged. The pointing error remains unchanged. Table 6 lists the estimated performance of an 8 m BIMA style dish with a CFRP feedleg(In this table feedleg pointing error using 1/12 th of the steel value, assuming the expansion of CFRP used is not zero.).

8. Thermal effects of yoke and base structures.

The above discussions deal with the performance of the steel dish plus feedleg. Thermal effects from other parts of the antenna, the yoke and pedastal will also influence pointing and phase. The sunshades used on the BIMA antenna help the problem but are not a complete solution. The advantages and disadvantage of the sunshades are:

1) Reflecting most of the solar radiation back to sky.
2) The air gap between sunshades will avoid over heating of the structure(when the structure is a lot hot or a lot cold than the ambient temperature).
3) The sunshade reduces greatly the convection heat exchange by the air or wind. this is

the disadvantage of the sunshades.

Temperature differences on the yoke structure will produce pointing errors in two ways. The first is the case when there is a temperature difference between one arm and the other of the yoke structure; the other is the case when there is a temperature difference between two sides of the yoke arm where the elevation encoder is located. By considering the first case, for a yoke of 1.5 m high and 2 m seperation, the pointing error is 1.7 arc sec/°C. To estimate the time required in building up a 1°C temperature difference, we could use the following assumption:

maximum solar loading	1260 W/m^2 (Note, this is an uper limit)
absorption of shiny sunshade	0.04 (Note, this is a lower limit including foam effect)
radiation factor to structure from sunshade	0.5
structure wall thickness	0.025 m
structure area factor *	2.4 (Note, assume a larger side is under the sun)
steel density	7800 kg/ m^3
steel specific heat	418 J/kg °C

* structure area factor is the ratio of the area under solar loading and the area where temperature incrases.

These values result in a solar loading on the structure of 25 W/m^2, the temperature increase for one arm is 199,000 J/°C(the conduction through the yoke bottom part is not considered, which is small when the temperature difference is small). This gives a temperature increase of one degree in 2.2 hours for one arm. Three hours of direct sunlight on one arm will result in a pointing error of 2.4 arc sec(0.8 arc sec rms). The rate of change is 0.4 arc sec(0.2 arc sec rms) for 30 minutes time.

In the second case the pointing error results from a twisting of the encoder body and in this case the parameters are the same except we need a larger structure area factor as the heat is coming from a small side of the arm. We use an area factor of 3 in the calculation to include half of the yoke arm. The heat required is 248,000 J/°C. Then the time it takes is 2.73 hours for a degree temperature difference between sides of an arm. In this part of calculation, we omit an important factor: conduction of side walls. The conduction of the side wall would be significant when the temperature difference is a little larger as the arm width is much smaller. So a correction factor of 0.5 is needed only for long term(3 hours) thermal pointing error. If the width of the arm top is 0.43 m, then the thermal pointing error is 15 arc sec/°C. For 3 hours sun shinning, the calculation results a temperature difference of 0.55°C(the factor of 0.5 is considered here for the conduction of heat from one side to the other.), the maximum pointing error is 8 arc sec(In table 7, 3 arc sec rms is used as yoke pointing error in 3 hours.). In short period of 30 minutes time, the temperature difference is 0.18°C, results in a pointing error of 2.6 arc sec(In table 7, 0.9 arc sec rms is used for yoke pointing error in 30 minutes.). This error is an important one in the total pointing error budget. However, a tilt meter may be used to correct this part of the error. The bottom part of the yoke and the base also contribute pointing errors as a temperature difference may build up between one side and the other. The concrete foundation has very small conductivity and relative large thermal expansion. In direct sunlight a temperature gradient may

build up and cause a large pointing error if the foundation is above the ground level. However this error may also be corrected by using a tilt meter.

The effect on phase error by other structural elements is added to the effects of dish and feedlegs. We use the same formula $3\ \delta_1 - 2\delta_2$ in the calculation. If the height of the antenna is 8 m, the δ_1 will be 96 μm for a 1°C temperature change in the antenna structure, and δ_2 will be 136 μm for steel feedleg(focal length is 3.36 m), when the antenna is pointing zenith. The net phase change will be 16 μm for a 1°C temperature change. When the dish is pointing at the horizen, δ_1 is small, eg. 24 μm(for 2 m distance from vertex to elevation axis), and δ_2 is 60 μm and the net error is 48 μm. However, if the feedleg is made of CFRP, the movements in the zenith pointing will be δ_1= 96 μm and δ_2= 56 μm and the net phase error is 176 μm. Taking a smaller rate of change for the structure temperature, 1.5°C/ hr, within a time period of 30 minutes, the structure expansion induced phase error is 0.75x176 = 132μm(In table 7, 44 μm rms is used as the yoke error in 30 minutes). The phase error in 3 hours is 6 times this number. This error will replace the phase error term of the dish absolute temperature change. In summary, Table 7 listed all of the thermal errors of the 8 m antenna, which has a steel backing struture and a CFRP feedleg.

Table 7 The thermal performance of a scaled 8 m steel antenna with CFRP feed leg design

	Surface Error	Pointing Error	Phase Error
Themal condition	rms dish deviation: 0.6°C cabin dish difference:1°C	rms dish deviation: 0.6°C feedleg difference: 1.5°C	rms dish deviation:0.6°C feeddish difference:1.5°C
Absolute error in 3 hours	dish error 24 μm cabin error 18.5 μm total rms 30 μm	dish error 0.4 arcsec rms feed error 0.1 arcsec rms yoke error3.0 arcsec rms total 3.0 arc sec	dish error 52 μm rms* yoke error 260μm rms feed error 95 μm rms total 280 μm rms
Absolute error in 30 minutes	dish error 24 μm cabin error 18.5 um total rms 30 μm	dish error 0.4 arcsec rms feed error 0.1 arcsec rms yoke error0.9 arcsec rms total 1.0 arcsec	dish error 52 μm rms* yoke error 44 μm rms feed error 95 μm rms total 115 μm rss
Rate of change	18 μm/ hr	1.0 arc sec /hr	230 μm/ hr
Error after calibration	24 μm rms	0.5 arc sec rms calibration every 30 min	12 μm rms calibration every 3 min

* This term is caused by the temperature spatial distribution on the dish.

8. Conclusions

The conventional antenna design using steel as the structural material has significant thermally

build up and cause a large pointing error if the foundation is above the ground level. However this error may also be corrected by using a tilt meter.

The effect on phase error by other structural elements is added to the effects of dish and feedlegs. We use the same formula $3\ \delta_1 - 2\delta_2$ in the calculation. If the height of the antenna is 8 m, the δ_1 will be 96 μm for a 1°C temperature change in the antenna structure, and δ_2 will be 136 μm for steel feedleg(focal length is 3.36 m), when the antenna is pointing zenith. The net phase change will be 16 μm for a 1°C temperature change. When the dish is pointing at the horizen, δ_1 is small, eg. 24 μm(for 2 m distance from vertex to elevation axis), and δ_2 is 60 μm and the net error is 48 μm. However, if the feedleg is made of CFRP, the movements in the zenith pointing will be δ_1= 96 μm and δ_2= 56 μm and the net phase error is 176 μm. Taking a smaller rate of change for the structure temperature, 1.5°C/ hr, within a time period of 30 minutes, the structure expansion induced phase error is 0.75x176 = 132μm(In table 7, 44 μm rms is used as the yoke error in 30 minutes). The phase error in 3 hours is 6 times this number. This error will replace the phase error term of the dish absolute temperature change. In summary, Table 7 listed all of the thermal errors of the 8 m antenna, which has a steel backing struture and a CFRP feedleg.

Table 7 The thermal performance of a scaled 8 m steel antenna with CFRP feed leg design

	Surface Error	Pointing Error	Phase Error
Themal condition	rms dish deviation: 0.6°C cabin dish difference:1°C	rms dish deviation: 0.6°C feedleg difference: 1.5°C	rms dish deviation:0.6°C feeddish difference:1.5°C
Absolute error in 3 hours	dish error 24 μm cabin error 18.5 μm total rms 30 μm	dish error 0.4 arcsec rms feed error 0.1 arcsec rms yoke error3.0 arcsec rms total 3.0 arc sec	dish error 52 μm rms* yoke error 260μm rms feed error 95 μm rms total 280 μm rms
Absolute error in 30 minutes	dish error 24 μm cabin error 18.5 um total rms 30 μm	dish error 0.4 arcsec rms feed error 0.1 arcsec rms yoke error0.9 arcsec rms total 1.0 arcsec	dish error 52 μm rms* yoke error 44 μm rms feed error 95 μm rms total 115 μm rss
Rate of change	18 μm/ hr	1.0 arc sec /hr	230 μm/ hr
Error after calibration	24 μm rms	0.5 arc sec rms calibration every 30 min	12 μm rms calibration every 3 min

* This term is caused by the temperature spatial distribution on the dish.

8. Conclusions

The conventional antenna design using steel as the structural material has significant thermally

induced errors affecting the pointing, surface accuracy and phase stability. The main contributions are from the dish and the yoke structure. The BIMA antenna uses a very effective dish thermal control system minimising the dish contribution. The yoke structure thermal control is less effective, giving rise to significant pointing errors. By frequent calibration of phase and pointing an 8 m dish of steel structure with CFRP feedleg can marginally satisfy the present requirements for the MMA antennas. This memo does not discuss the wind and the errors introduced by bearing toerances.

9. Acknowledgements.

Thanks to the MMA Antenna Working Group.

References.

D. Woody et al, Design, construction, and performance of the Leighton 10.4 m diameter radio telescopes, Proc. IEEE, 82, 673, 1994.

J. W. Lamb and J. R. Forster, Temperature measurements on BIMA 6 m antennas-part 1: backing structure, mmA memo, NRAO, 1993.

A. Greve, Thermal design and thermal behaviour of radio telescope structures, IRAM, 1992.

J.D. Bregman and J.L. Casse, A simulation of the thermal behaviour of the UK-NL millimeter wave telescope, Intern. J. of Infrared and Millimeter Waves. 6, 25, 1985.

J. Cheng, Slant-axis antenna design II, mmA memo, NRAO, 1994.

Figure 1 Measured average temperature and rms deviation of the temperature of the BIMA backing structure(from Lamb and Forster).

Figure 2 Measured temperature data of the BIMA antenna backing structure in hours of a day(from Lamb and Forster).

Figure 3 Drawing of BIMA backing structure truss showing location of thermistors(from Lamb and Forster).

Figure 4 RMS temperature deviation of IRAM 30 m antenna backing structure(from Greve).

Figure 5 Temperature variation of the panel and the ambient air(dotted line) of IRAM 30 m antenna(Fig.2.4 of Greve(1992)).

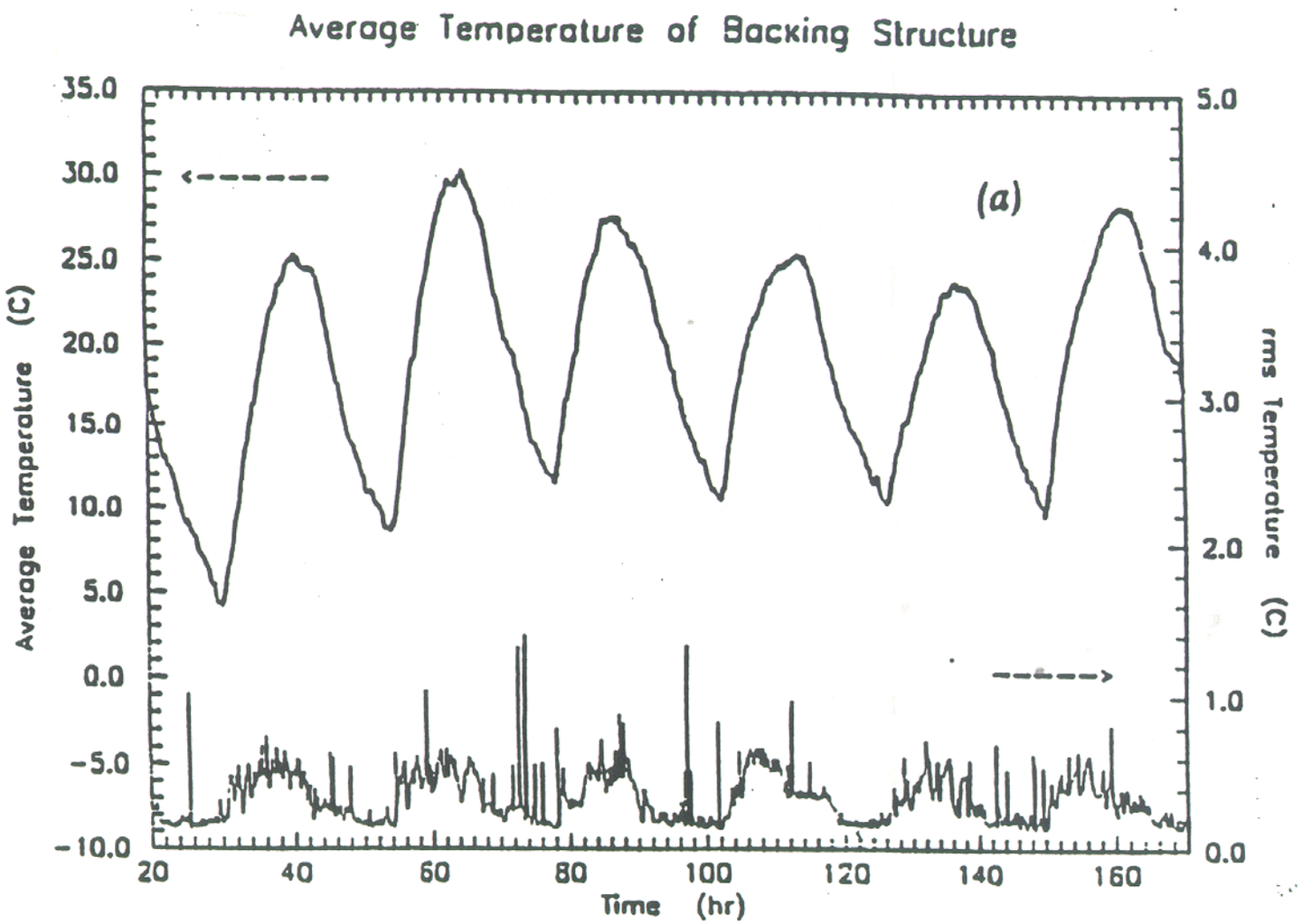

Figure 1 Measured average temperature and rms deviation of the temperature of the BIMA backing structure(from Lamb and Forster).

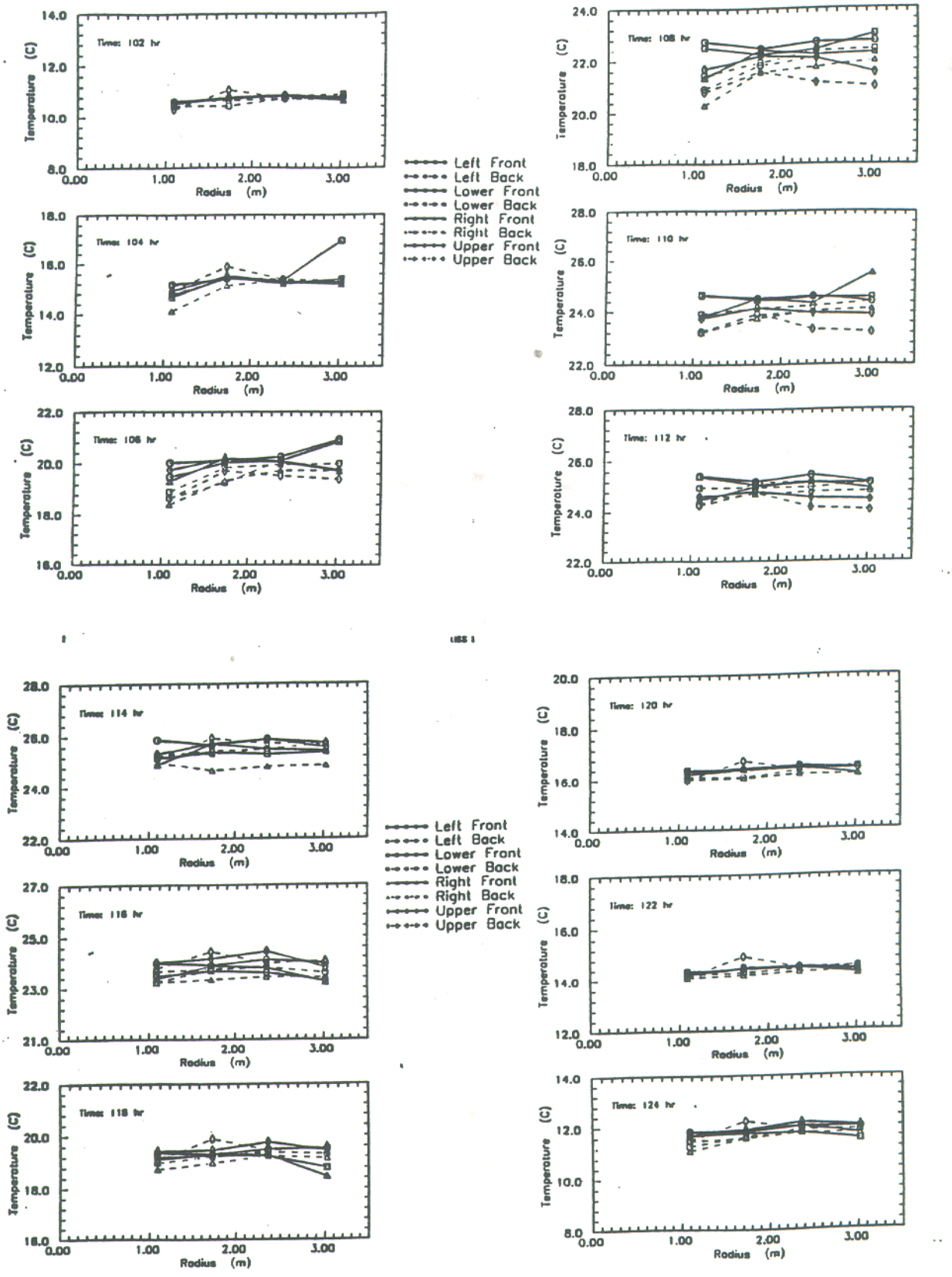

Figure 2 Measured temperature data of the BIMA antenna backing structure in hours of a day(from Lamb and Forster).

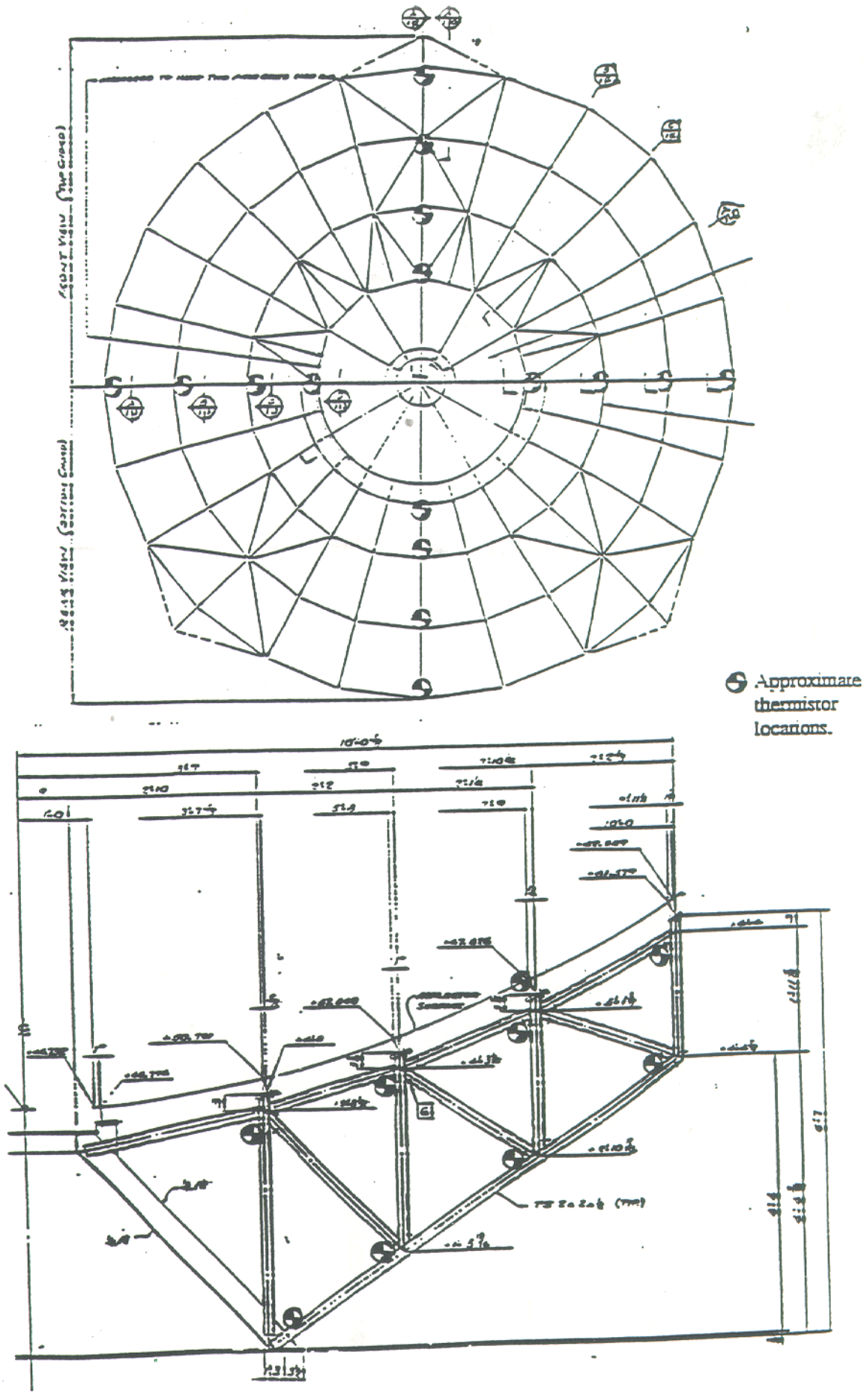

Figure 3 Drawing of BIMA backing structure truss showing location of thermistors(from Lamb and Forster).

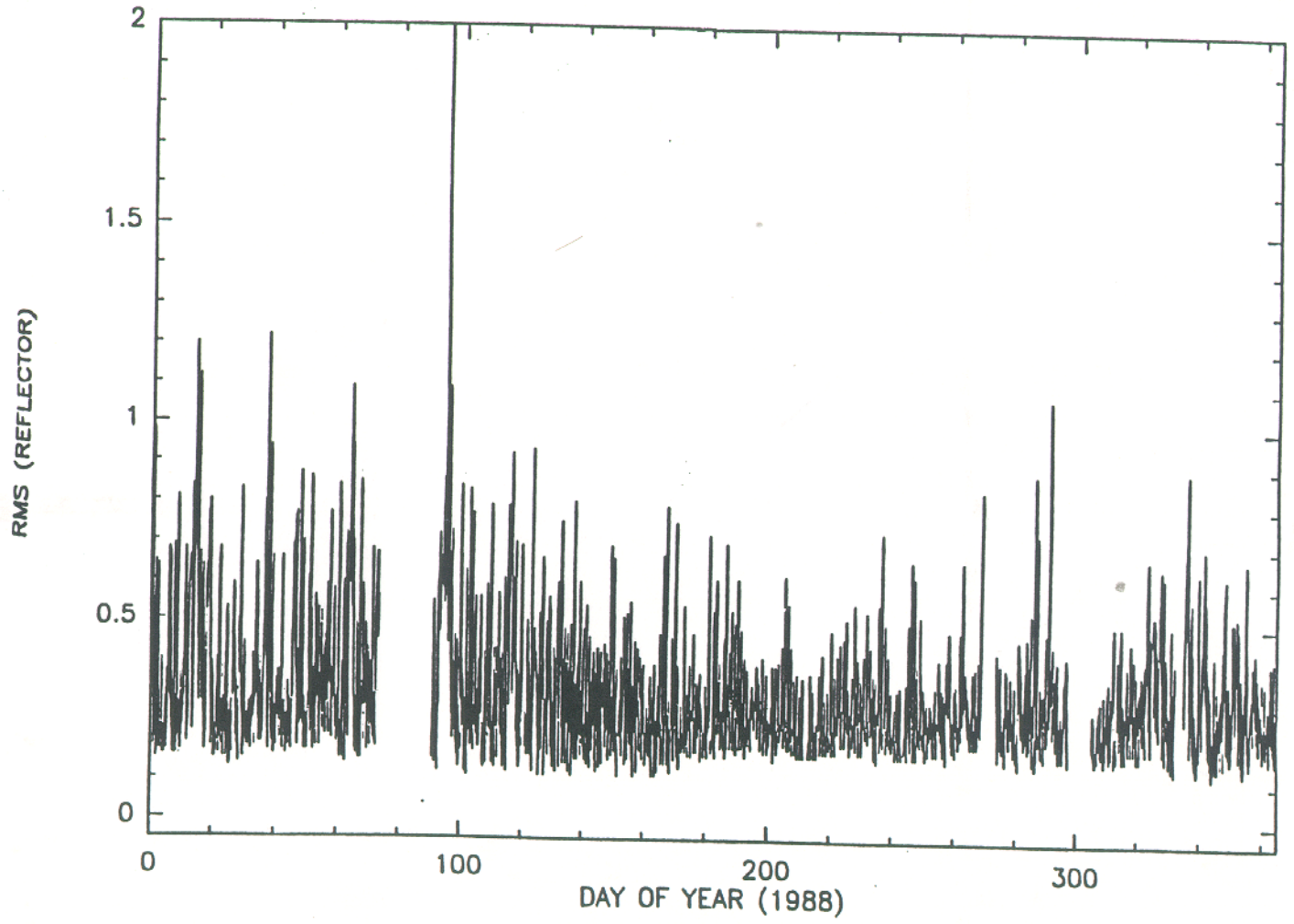

Figure 4 RMS temperature deviation of IRAM 30 m antenna backing structure(from Greve).

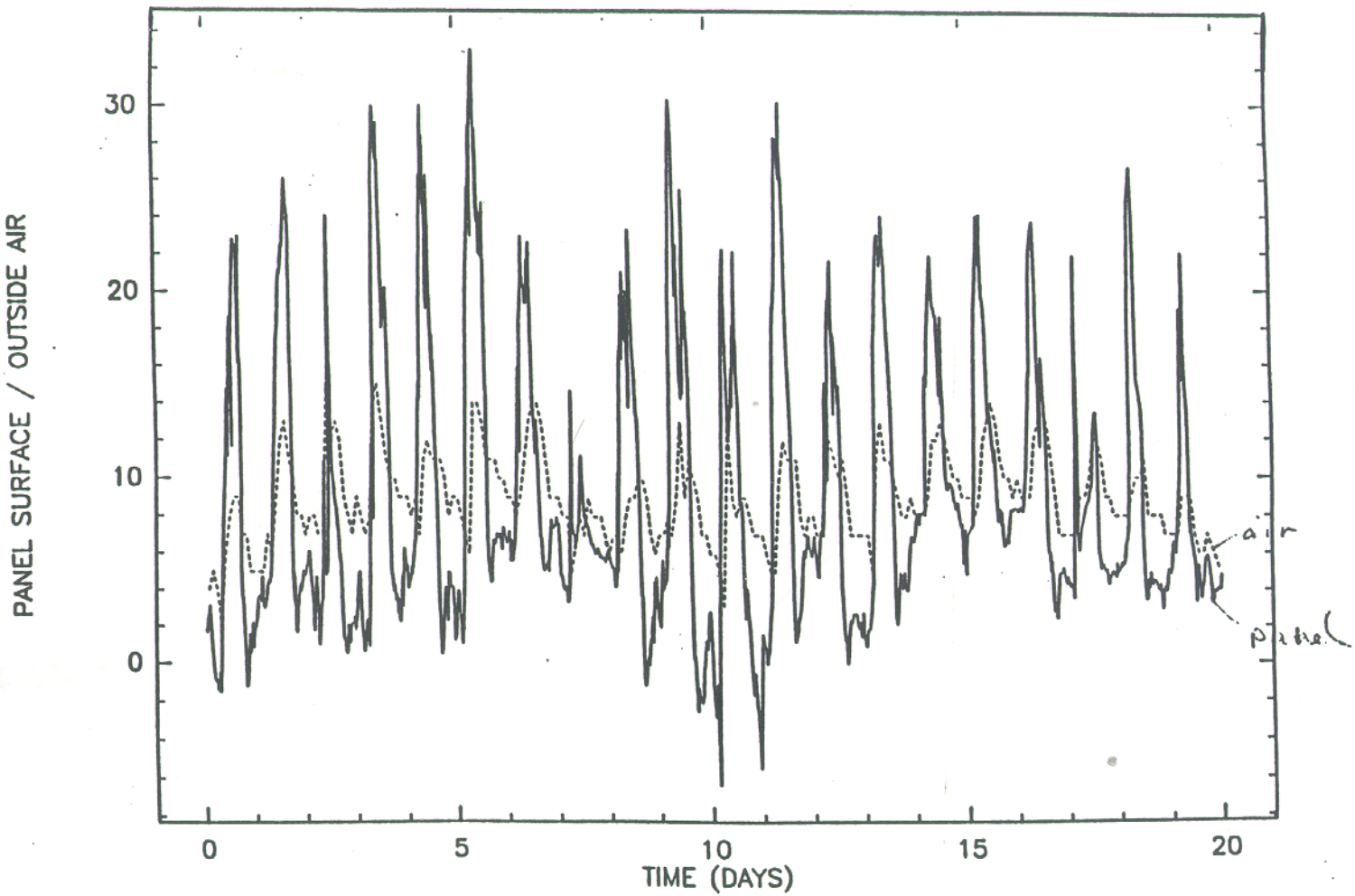

Figure 2.4

Recorded temperature variation of a panel front surface (solid line) measured on the IRAM 30 m telescope and temperature variation of the ambient air (dashed line). Thermal control of the telescope working.

Figure 5 Figure 2.4 of Greve report, 1992 on panel and ambient temperature data.